7(2010) 167 – 183

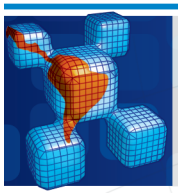

Latin American Journal of Solids and Structures
www.lajss.org

The use of piezoelectric stress stiffening to enhance buckling of laminated plates

Abstract

A technique for enhancement of buckling loads of composite plates is proposed. The technique relies on using stress stiffening to create a non-zero tensile force acting along the plate plane which ultimately permits the application of higher external compressive forces that lead to traditional buckling instabilities. The idea is to completely restrain the plate movements in its plane direction, at all edges, and to apply voltages to pairs of symmetrically bonded piezoelectric patches. This voltage is applied such that the piezoelectric patches contract resulting in a uniform tensile force over the plate plane.

Keywords

buckling, piezoelectric, stress stiffening, composites

Alfredo R. de Faria[a,*] **and Maurício V. Donadon**[b]

[a] Instituto Tecnológico de Aeronáutica, CTA - ITA - IEM, São José dos Campos, SP 12228-900, Tel.: 55-12-39475901; fax: 55-12-39475967 – Brazil

[b] Instituto Tecnológico de Aeronáutica, CTA - ITA - IEA, São José dos Campos, SP 12228-900, Tel.: 55-12-39475944; fax: 55-12-39475824 – Brazil

Received 27 Nov 2009;
In revised form 24 Mar 2010

* Author email: arfaria@ita.br

1 INTRODUCTION

Buckling of laminated plates caused by several types of loadings (mechanical, thermal, etc.) is one of the most relevant problems encountered in the area of composite structures. One technique available to increase buckling loads of this type of structure is to incorporate active elements, sensors and actuators, and control systems to such structures. Hence, these systems composed of host composite structure, active elements and control may have their buckling load increased with respect to the buckling load of the host structure if isolatedly considered.

A number of materials and devices are available to implement active control. However, piezoelectric materials are again gaining popularity since their boom in the eighties [4] and nineties [10, 14]. Several investigations using the electromechanical properties of these materials are concerned with active control of vibrations, noise suppression, flutter control, shape control and buckling load optimization.

Chandrashenkhara and Bathia [3] presented a finite element formulation to study the stability of laminated plates with integrated piezoelectric sensors and actuators. The finite element model is based on the theory of Reissner-Mindlin.

Meressi and Paden [10] derived the linearized equation of motion of a simply supported flexible beam with piezoelectric actuators and subjected to several conditions of axial loading.

They concluded that the buckling load of this beam could be greater than the buckling load of the same beam without the action of the elements piezoelectric. Refined plate theories that account for piezoeletric effects are available in Refs. [2, 8]. A survey of such theories can be found in Ref. [7]. These refined theories address specially the kinematic relations in the displacement and electric fields. However, for the present work, a thin composite plate suited for aerospace applications is modeled and investigated. Hence, the theoretical formulation of laminated plates with layers of piezoelectric actuators and sensors using the Reissner-Mindlin plate theory contained in Ref. [12] shall be adopted.

Donadon *et al.* [6] investigated the efficiency of the use of piezoelectric elements in the enhancement of natural frequencies of laminated plates. A finite element formulation was proposed for the analysis of laminated plates with an arbitrary number of piezoelectric actuators and sensors. Nonlinear strain × displacement von Karman relations were used and a linear behavior was assumed for the electric degrees of freedom. Different configurations were analyzed both numerically and experimentally. The piezoelectric stress stiffening effect, also considered in the present work, is used to increase natural frequencies of composite plates.

de Faria [5] proposed the use of piezoelectric stiffening stresses to create a nonzero traction force acting along the axis of a laminated beam, allowing the application of an external compressive force greater than the buckling load of this beam without the presence of piezoelectric actuators. It was shown that the actuators' length interfere with the intensity of the traction force piezoelectrically induced. However, the position of these actuators along the length of the beam does not alter the intensity of the traction force.

Kundun *et al.* [9] used the theory of nonlinear large deformations to study post-buckling of piezoelectric laminated shells with double curvature through the finite element method. Batra and Geng [1] and Shariyat [13] present proposals to enhance dynamic buckling of flexible plates.

The prebuckling enhancement of composite plates equipped with piezoelectric actuators is the subject of this paper. Piezoelectric actuators are used to induce in-plane traction stiffening stresses in a composite plate, thereby counteracting external compressive stresses that render the structure unstable. The objective is to create in-plane piezoelectric stiffening stresses to enhance buckling loads of laminated plates. The idea is to completely restrain in-plane displacements on its boundary and to apply voltage to piezoelectric actuators symmetrically bonded to the top and bottom surfaces. This voltage is applied such that the piezoelectric actuators shrink generating traction stresses in the plate plane. Therefore, if external compressive stresses destabilize the structure the stiffening piezoelectric traction stresses will act, re-stabilizing the structure. Analytical approximations and the finite element method are used to compute the piezoelectric stiffening stresses whereas the finite element method is used to solve the buckling problem. The results presented consider bifurcation buckling, although the formulation proposed is general enough to be applicable for nonlinear analysis and critical point type of buckling.

2 PROBLEM FORMULATION

The equations that describe the electromechanical behavior of a plate containing layers of the piezoelectric actuators bonded on its top and bottom surfaces are presented. The buckling analysis of the laminated plate is based on the Mindlin plate theory and the electric potential is assumed constant over the surface of the piezoelectric layers and varying linearly along the thickness of these layers.

The basic configuration of the host structure consists of a rectangular plate equipped with patches of piezoelectric actuators symmetrically bonded to the top and bottom surfaces. Figure 1 shows three situations where there are pairs of piezoelectric actuators bonded to the bottom and top plate surface. In the prebuckling phase, only in-plane displacements and stresses arise. When nonzero voltages are equally applied to the top and bottom piezoelectric patches displacements u and v result. In this phase the boundary conditions assumed are that of completely constrained edges with $u = v = 0$. If the plate's edges were free to move then there would be no piezoelectric stiffening stresses. Once the piezoelectric patches are energized traditional mechanical forces uniformly distributed along the edges and usually denoted by N_{xx0}, N_{yy0}, N_{xy0} are slowly applied causing compressive and shear stresses that eventually buckle the plate. In a testing facility forces N_{xx0}, N_{yy0}, N_{xy0} would possibly be the result of prescribed displacements.

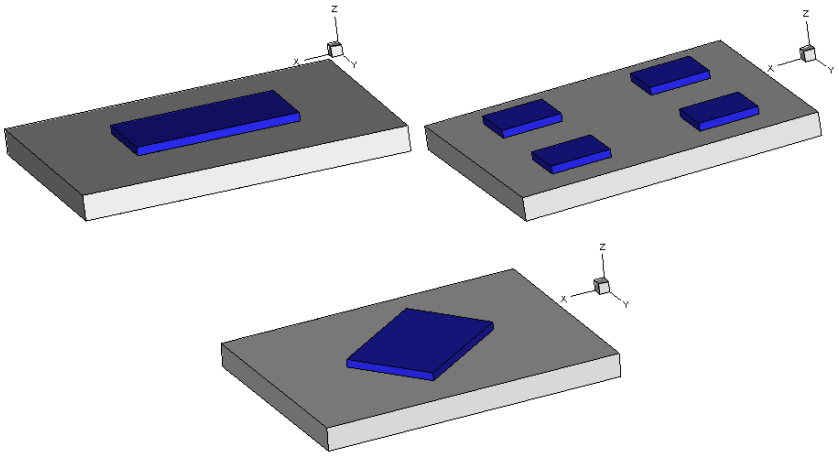

Figure 1 Basic configurations

The constitutive equations can be written as in Eq. (1) where it is assumed that the piezoelectric layers are polarized along the z direction (perpendicular to the plate).

$$\boldsymbol{\sigma} = \overline{\mathbf{Q}}\boldsymbol{\epsilon} - \mathbf{e}^T\mathbf{E}, \quad \boldsymbol{\tau} = \overline{\mathbf{Q}}_S\boldsymbol{\gamma}, \quad \mathbf{d} = \mathbf{e}\boldsymbol{\epsilon} + \boldsymbol{\xi}\mathbf{E}, \tag{1}$$

where $\overline{\mathbf{Q}}$ is the ply in-plane stiffness matrix in the structural coordinate system, $\overline{\mathbf{Q}}_S$ is the ply out-of-plane shear stiffness matrix in the structural coordinate system, $\boldsymbol{\sigma}$ are in-plane stresses, $\boldsymbol{\tau}$ are out-of-plane shear stresses, $\boldsymbol{\epsilon}$ are the in-plane strains including nonlinear components, $\boldsymbol{\epsilon}$

are the out-of-plane shear srains, $\mathbf{d}$ is the electric displacement, $\mathbf{E}$ is the electric field, $\mathbf{e}$ is the electro-mechanical coupling matrix and $\boldsymbol{\xi}$ is the permitivitty matrix. Notice that $\boldsymbol{\tau}$ is free of piezoelectric effects [8]. Equation (1) is valid in general for both composite and piezoelectric material. In the case of a composite layer matrices $\mathbf{e}$ and $\boldsymbol{\xi}$ would vanish.

The system is conservative such that the total potential energy is given by:

$$\Pi = \frac{1}{2}\int_V \boldsymbol{\sigma}^T \boldsymbol{\epsilon} dV + \frac{1}{2}\int_V \boldsymbol{\tau}^T \boldsymbol{\gamma} dV - \frac{1}{2}\int_V \mathbf{d}^T \mathbf{E} dV - W, \tag{2}$$

where W is the work of external forces N_{xx0}, N_{yy0}, N_{xy0}.

The Mindlin plate displacement field is now introduced:

$$\begin{aligned} \tilde{u}(x,y,z) &= u(x,y) + z\psi_x(x,y), \\ \tilde{v}(x,y,z) &= v(x,y) + z\psi_y(x,y), \\ \tilde{w}(x,y,z) &= w(x,y), \end{aligned} \tag{3}$$

where $\tilde{u}$, $\tilde{v}$, $\tilde{w}$ are the displacements of an arbitrary point in the plate, u, v, w are the mid plane displacements ($z = 0$) and ψ_x, ψ_y are the mid plane rotations. The strains $\boldsymbol{\epsilon}$ can now be split into three components: membrane strains $\boldsymbol{\epsilon}_0$, curvature $\boldsymbol{\kappa}$ and nonlinear von Karman strains $\boldsymbol{\epsilon}_N$ such that

$$\boldsymbol{\epsilon} = \boldsymbol{\epsilon}_0 + z\boldsymbol{\kappa} + \boldsymbol{\epsilon}_N = \left\{ \begin{array}{c} u_{,x} \\ v_{,y} \\ u_{,y} + v_{,x} \end{array} \right\} + z \left\{ \begin{array}{c} \psi_{x,x} \\ \psi_{y,y} \\ \psi_{x,y} + \psi_{y,x} \end{array} \right\} + \frac{1}{2} \left\{ \begin{array}{c} w_{,x}^2 \\ w_{,y}^2 \\ 2w_{,x}w_{,y} \end{array} \right\},$$

$$\boldsymbol{\gamma} = \left\{ \begin{array}{c} w_{,x} + \psi_x \\ w_{,y} + \psi_y \end{array} \right\}. \tag{4}$$

In order to facilitate manipulation of Eq. (2) matrices $\mathbf{A}$, $\mathbf{B}$, $\mathbf{D}$ and $\mathbf{A}_S$, and vectors $\mathbf{N} = \{ \; N_{xx} \quad N_{yy} \quad N_{xy} \; \}^T$, $\mathbf{M} = \{ \; M_{xx} \quad M_{yy} \quad M_{xy} \; \}^T$, $\mathbf{Q} = \{ \; Q_{xx} \quad Q_{yy} \; \}^T$ and $\mathbf{F} = \{ \; F_{xx} \quad F_{yy} \quad F_{xy} \; \}^T$ are defined as

$$\begin{aligned} (\mathbf{A}, \mathbf{B}, \mathbf{D}) &= \int_{-h/2}^{h/2} (1, z, z^2) \overline{\mathbf{Q}} dz \\ \mathbf{A}_S &= \int_{-h/2}^{h/2} \overline{\mathbf{Q}}_S dz \\ \mathbf{F} &= \int_{-h/2}^{h/2} \mathbf{e}^T \mathbf{E} dz \\ \left\{ \begin{array}{c} \mathbf{N} \\ \mathbf{M} \end{array} \right\} &= \left[\begin{array}{cc} \mathbf{A} & \mathbf{B} \\ \mathbf{B} & \mathbf{D} \end{array} \right] \left\{ \begin{array}{c} \boldsymbol{\epsilon}_0 + \boldsymbol{\epsilon}_N \\ \boldsymbol{\kappa} \end{array} \right\} \\ \mathbf{Q} &= \mathbf{A}_S \boldsymbol{\gamma}, \end{aligned} \tag{5}$$

where h is the total thickness. Following conventional terminology, the components of $\mathbf{N}$ are the in-plane forces per unit length, the components of $\mathbf{Q}$ are the out-of-plane shear forces per unit length, the components of $\mathbf{F}$ are the piezoelectric in-plane forces per unit length and the components of $\mathbf{M}$ are bending moments per unit length. From this point on these will be simply referred to as forces or moments. Notice that the piezoelectric layers make a contribution to the laminate stiffness matrices $\mathbf{A}$, $\mathbf{B}$, $\mathbf{D}$ and $\mathbf{A}_S$. On the other hand, vector $\mathbf{F}$ is nonzero only if there are piezoelectric layers present in the laminate. $\mathbf{F}$ can be interpreted as the piezoelectric force. If the electric field E_z is replaced by ϕ/t where ϕ is voltage and t is thickness then Eq. (5c) can be specialized to become [11]

$$\left\{ \begin{array}{c} F_{xx} \\ F_{yy} \\ F_{xy} \end{array} \right\} = \left\{ \begin{array}{c} e_{31}(\phi_T + \phi_B) \\ e_{32}(\phi_T + \phi_B) \\ 0 \end{array} \right\}, \tag{6}$$

where ϕ_T and ϕ_B are the voltages applied to the top and bottom surfaces of the plate. In practical applications $e_{32} = e_{31}$ what leads to $F_{xx} = F_{yy}$.

Taking the first variation of Eq. (2), assuming that the voltages are prescribed and integrating through the thickness yields

$$\begin{aligned} \delta\Pi = \int_\Omega (\mathbf{N}^T\delta\boldsymbol{\epsilon}_0 + \mathbf{N}^T\delta\boldsymbol{\epsilon}_N + \mathbf{M}^T\delta\boldsymbol{\kappa} + \mathbf{Q}^T\delta\boldsymbol{\gamma} - \mathbf{F}^T\delta\boldsymbol{\epsilon}_0 - \mathbf{F}^T\delta\boldsymbol{\epsilon}_N)d\Omega - \\ \int_\Gamma (N_{xx0}, N_{xy0})\cdot\vec{n}\,\delta u d\Gamma - \int_\Gamma (N_{xy0}, N_{yy0})\cdot\vec{n}\,\delta v d\Gamma = 0, \end{aligned} \tag{7}$$

where Ω is the in-plane plate domain, N_{xx0}, N_{yy0}, N_{xy0} are membrane forces applied along the plate edge Γ (the boundary of Ω), $\vec{n}$ is the unit vector normal to Γ and the term containing $z\mathbf{F}^T\delta\boldsymbol{\kappa}$ was abandoned since full symmetry ($\phi_T = \phi_B$) has been admitted. Notice that if $\phi_T \neq \phi_B$ then the prebuckling problem would result in nonzero out-of-plane displacements ($w \neq 0$) and no bifurcation type buckling would occur.

Substitution of Eqs. (4) into Eq. (7) and integration by parts in two dimensions allows one to obtain the governing equations

$$\begin{aligned} (N_{xx} - F_{xx})_{,x} + (N_{xy} - F_{xy})_{,y} = 0 \\ (N_{xy} - F_{xy})_{,x} + (N_{yy} - F_{yy})_{,y} = 0 \\ M_{xx,x} + M_{xy,y} = Q_{xx} \\ M_{yy,y} + M_{xy,x} = Q_{yy} \\ Q_{xx,x} + Q_{yy,y} + (N_{xx} - F_{xx})w_{,xx} + (N_{yy} - F_{yy})w_{,yy} + 2(N_{xy} - F_{xy})w_{,xy} = 0 \end{aligned} \tag{8}$$

and in-plane boundary conditions valid on the plate's edges:

$$\begin{aligned} (N_{xx} - F_{xx}, N_{xy} - F_{xy})\cdot\vec{n}\,\delta u &= (N_{xx0}, N_{xy0})\cdot\vec{n}\,\delta u \\ (N_{xy} - F_{xy}, N_{yy} - F_{yy})\cdot\vec{n}\,\delta v &= (N_{xy0}, N_{yy0})\cdot\vec{n}\,\delta v. \end{aligned} \tag{9}$$

Notice that there are three more boundary conditions related to δw, $\delta\psi_x$, $\delta\psi_y$ that, although indispensable to solve the buckling eigenproblem, are not given in Eq. (9).

Terms $(N_{xx} - F_{xx})$, $(N_{xy} - F_{xy})$ and $(N_{yy} - F_{yy})$ present in Eqs. (8) and (9) correspond to the piezoelectric stiffening stress resultants. Hence, if there are no piezoelectric stiffening stresses then buckling cannot occur due to the piezoelectric effect. There are two possibilities for buckling to occur: (i) external mechanical forces N_{xx0}, N_{yy0} or N_{xy0} must be present (this is the traditional buckling problem) and (ii) nonzero piezoelectric stiffening stresses must exist. Situation (ii) is the subject of next section.

3 PIEZOELECTRIC STIFFENING STRESSES

In order to obtain the piezoelectric stiffening stress distribution it is necessary to solve the prebuckling Eqs. (8a) and (8b) along with their boundary conditions in Eq. (9). Unfortunately, this problem does not admit an exact analytical solution mainly because of the discontinuity caused by the presence of piezoelectric patches bonded to the plate surfaces. The patches are source of two kinds of discontinuity: stiffness and piezoelectric force. It is clear that adding piezoelectric layers to the laminate increases the in-plane stiffness matrix $\mathbf{A}$. It is also clear that the piezoelectric forces F_{xx}, F_{yy}, F_{xy} are nonzero only when piezoelectric patches are attached, that is, over the regions of the plate where there are no actuators $F_{xx} = F_{yy} = F_{xy} = 0$.

The bifurcation type buckling is the subject of this paper. The objective is to enhance the critical buckling load of plates that exhibit such type of buckling by appropriately tailoring the piezoelectric stiffening stresses. Therefore, this study is concerned with cases where there are no out-of-plane displacements w in the prebuckling regime. This can only be achieved when there is full symmetry on the actuators part ($\phi_T = \phi_B$) and when the laminate is symmetric ($\mathbf{B} = \mathbf{0}$ and $t_T = t_B$). If these conditions apply and the nonlinear strain components are neglected in the prebuckling regime then Eq. (7) can be simplified to:

$$\delta\Pi = \int_\Omega \begin{Bmatrix} \delta u_{,x} \\ \delta v_{,y} \\ \delta u_{,y} + \delta v_{,x} \end{Bmatrix}^T \left(\begin{bmatrix} A_{11} & A_{12} & A_{16} \\ A_{12} & A_{22} & A_{26} \\ A_{16} & A_{26} & A_{66} \end{bmatrix} \begin{Bmatrix} u_{,x} \\ v_{,y} \\ u_{,y} + v_{,x} \end{Bmatrix} - \begin{Bmatrix} F_{xx} \\ F_{yy} \\ F_{xy} \end{Bmatrix} \right) d\Omega = 0. \tag{10}$$

Analytical solution of Eq. (10) is not possible. However, it is possible to gain insight into the problem if a symmetric configuration is investigated. Assume that only one rectangular piezoelectric patch is placed in the center of the plate such as depicted in Fig. 2. Taking $u(x, y)$ as the displacements along x and $v(x, y)$ as the displacements along y the symmetry and boundary conditions are:

- Edge $y = 0$: $v(x, 0) = v_{,x}(x, 0) = v_{,xx}(x, 0) = ... = 0$, $u_{,y}(x, 0) = 0$;
- Edge $x = 0$: $u(0, y) = u_{,y}(0, y) = u_{,yy}(0, y) = ... = 0$, $v_{,x}(0, y) = 0$;
- Edge $y = L_y$: $v(x, L_y) = v_{,x}(x, L_y) = v_{,xx}(x, L_y) = ... = 0$, $u_{,y}(x, L_y) = 0$;
- Edge $x = L_x$: $u(L_x, y) = u_{,y}(L_x, y) = u_{,yy}(L_x, y) = ... = 0$, $v_{,x}(L_x, y) = 0$.

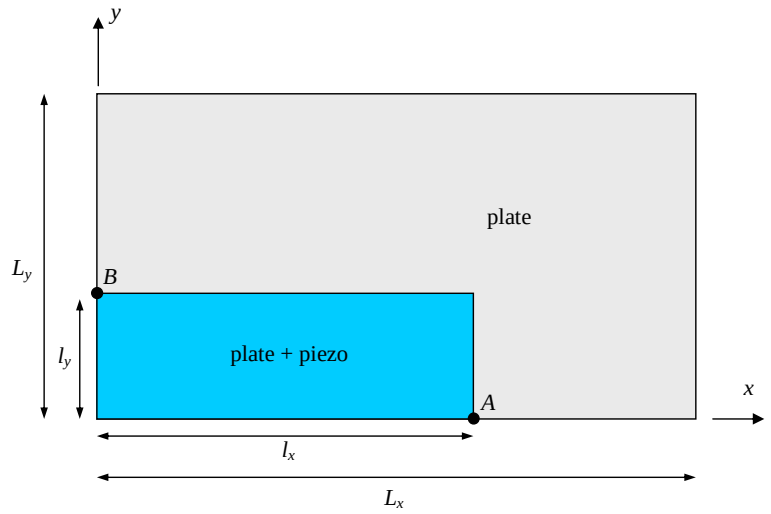

Figure 2 Basic dimensions

Conditions $v(x,0) = 0$, $u(0,y) = 0$, $u_{,y}(x,0) = 0$, $v_{,x}(0,y) = 0$ follow from the symmetry of the problem. $v(x,L_y) = 0$ and $u(L_x,y) = 0$ are enforced boundary conditions. $u_{,y}(x,L_y) = 0$ and $v_{,x}(L_x,y) = 0$ result from the requirements that $N_{xy}(x,L_y) = N_{xy}(L_x,y) = 0$ for a balanced laminate ($A_{16} = A_{26} = 0$) as given in Eq. (9). The boundary condition in Eq. (9) also imposes that continuity on $N_{xx} - F_{xx}$ and $N_{xy} - F_{xy}$ along any line of constant y must be satisfied as well as continuity on $N_{xy} - F_{xy}$ and $N_{yy} - F_{yy}$ along any line of constant x. Moreover, continuity of displacements u and v throughout must be observed.

Considering the lines $y = 0$, $x = 0$ and a balanced laminate, the continuity conditions on $N_{xx} - F_{xx}$ for point A and $N_{yy} - F_{yy}$ for point B read, respectively,

$$\begin{aligned} A^*_{11}u^*_{,x}(l_x,0) + A^*_{12}v^*_{,y}(l_x,0) - F_{xx} &= A_{11}u_{,x}(l_x,0) + A_{12}v_{,y}(l_x,0), \\ A^*_{12}u^*_{,x}(0,l_y) + A^*_{22}v^*_{,y}(0,l_y) - F_{yy} &= A_{12}u_{,x}(0,l_y) + A_{22}v_{,y}(0,l_y). \end{aligned} \tag{11}$$

where the terms with a superscript star ($*$) refer to domain where there are both plate and piezoelectric materials. From Eqs. (11) it can be seen that there must be discontinuity on $u_{,x}(x,0)$ and $v_{,y}(0,y)$. A finite element that enforces continuity on the first derivatives of u and v, such as the one based on the classical plate theory, would not be a good choice in this case. A better suited element for this task is the one based on Mindlin assumptions that are able to capture discontinuities on the first derivatives of u and v, whose description is in the next section.

Since exact solutions to Eq. (10) cannot be obtained it remains to find analytical approximations or numerical solutions. One approach to obtain approximations is to consider that the plate shown in Fig. 2 behaves similarly to a beam, at least along the lines $y = 0$, $x = 0$. Notice that this assumption implies ignoring Poisson effects that may be relevant in plate

problems. Therefore, the governing differential equations can be simplified to $u_{,xx}(x,0) = 0$ and $v_{,yy}(0,y) = 0$. Moreover, Eqs. (11) reduce to

$$\begin{aligned} A_{11}^{*} u_{,x}^{*}(l_x,0) - F_{xx} &= A_{11} u_{,x}(l_x,0), \\ A_{22}^{*} v_{,y}^{*}(0,l_y) - F_{yy} &= A_{22} v_{,y}(0,l_y). \end{aligned} \tag{12}$$

Considering the boundary conditions $u(0,0) = u(L_x,0) = 0$ and $v(0,0) = v(0,L_y) = 0$, and the jump conditions in Eq. (12), the differential equations $u_{,xx}(x,0) = 0$ and $v_{,yy}(0,y) = 0$ are solved to yield:

$$\begin{aligned} u^{*}(x,0) &= \frac{\left(\frac{1}{L_x} - \frac{1}{l_x}\right) x F_{xx}}{\left[A_{11}^{*}\left(\frac{1}{L_x} - \frac{1}{l_x}\right) - A_{11}\frac{1}{L_x}\right]} \quad , \quad u(x,0) = \frac{\left(\frac{x}{L_x} - 1\right) F_{xx}}{\left[A_{11}^{*}\left(\frac{1}{L_x} - \frac{1}{l_x}\right) - A_{11}\frac{1}{L_x}\right]}, \\ v^{*}(0,y) &= \frac{\left(\frac{1}{L_y} - \frac{1}{l_y}\right) y F_{yy}}{\left[A_{22}^{*}\left(\frac{1}{L_y} - \frac{1}{l_y}\right) - A_{22}\frac{1}{L_y}\right]} \quad , \quad v(0,y) = \frac{\left(\frac{y}{B} - 1\right) F_{yy}}{\left[A_{22}^{*}\left(\frac{1}{L_y} - \frac{1}{l_y}\right) - A_{22}\frac{1}{L_y}\right]}. \end{aligned} \tag{13}$$

The piezoelectric stiffening stress resultants are given by:

$$\begin{aligned} T_{xx} &= A_{11}^{*} u_{,x}^{*}(x,0) - F_{xx} = A_{11} u_{,x}(x,0) = \frac{F_{xx}}{\frac{A_{11}^{*}}{A_{11}}\left(1 - \frac{L_x}{l_x}\right) - 1}, \\ T_{yy} &= A_{22}^{*} v_{,y}^{*}(0,y) - F_{yy} = A_{22} v_{,y}(0,y) = \frac{F_{yy}}{\frac{A_{22}^{*}}{A_{22}}\left(1 - \frac{L_y}{l_y}\right) - 1}. \end{aligned} \tag{14}$$

A numerical example requires physical properties given in Tab. 1 and geometric parameters. The plate is assumed to have semi-length $L_x = 0.2$ m, semi-width $L_y = 0.15$ m. The piezoelectric actuator has semi-length $l_x = 0.15$ m and semi-width $l_y = 0.05$ m. A cross-ply laminate $[0/90]_S$ is used with each layer 0.15 mm thick. The thickness of the piezoelectric actuators (top and bottom) is 0.05 mm. A voltage of $\phi_T = \phi_B = 50$ V is applied which corresponds exactly to the depoling field in Tab. 1.

Figures 3 and 4 present a comparison between the analytical solutions given in Eq. (13) and the FE numerical solution, where $\xi = x/L_x$ and $\eta = y/L_y$. It is clear that the analytical solution along $y = 0$ is a very good approximation to the actual displacements. Both u and $u_{,x}$ agree well. However, the same is not true for analytical solution along $x = 0$. It can be observed that, although the patterns for v and $v_{,y}$ are similar in shape, their magnitudes are completely dispair. The conclusion is that, in this particular configuration, the plate behaves much like a beam in the x direction but not in the y direction.

Closer observation of Eq. (14) reveals that the piezoelectric stiffening stress resultants depend basically on two parameters: the relative stiffness $a = A_{11}^{*}/A_{11}$ and the nondimensional actuator length l_x/L_x. In the particular example selected $a = 1.14$ and $l_x/L_x = 0.75$. Figure

Table 1 Physical properties

Property	G1195N	T300/5208
Young modulus E_{11} (GPa)	63.0	154.5
Young modulus E_{22} (GPa)	63.0	11.13
Poisson ratio ν_{12}	0.3	0.304
Shear modulus $G_{12} = G_{13}$ (GPa)	24.2	6.98
Shear modulus G_{23} (GPa)	24.2	3.36
Piezoelectric constant e_{31} (N/V m)	17.6	-
Piezoelectric constant e_{32} (N/V m)	17.6	-
Depoling field E_{MAX} (V/mm)	1000	-

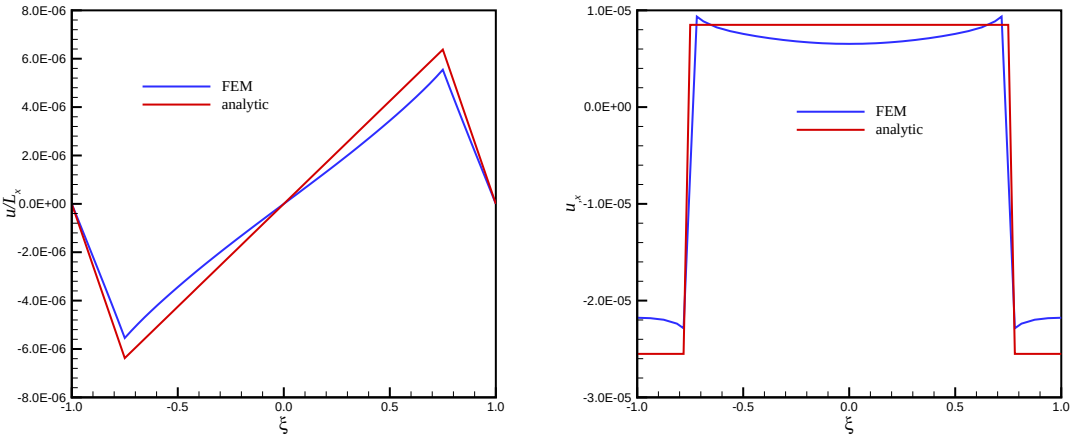

Figure 3 Comparison FEM vs. analytical solutions along $y = 0$

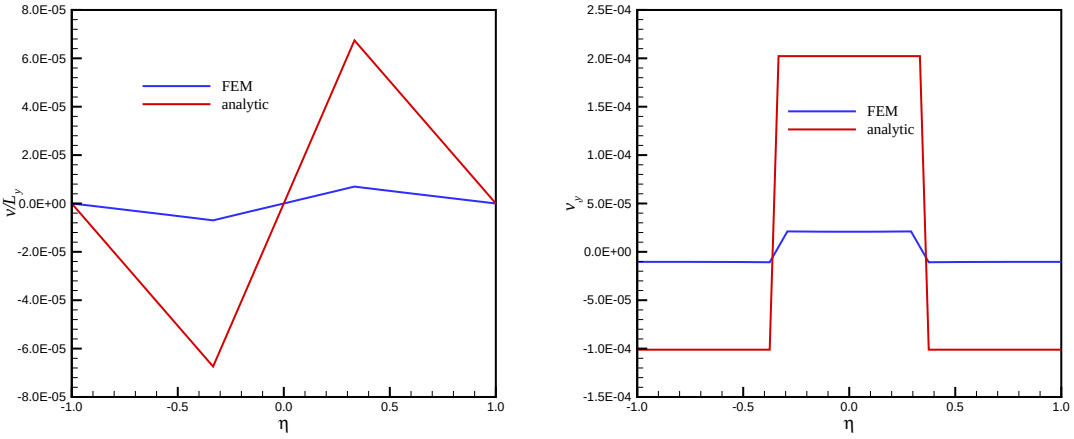

Figure 4 Comparison FEM vs. analytical solutions along $x = 0$

5 shows that, the smaller a, the greater is the efficiency to generate piezoelectric stiffening stresses. Fortunately, in aerospace applications, thin piezoelectric actuators are used leading to practical situations where $1.0 < a \leq 1.2$.

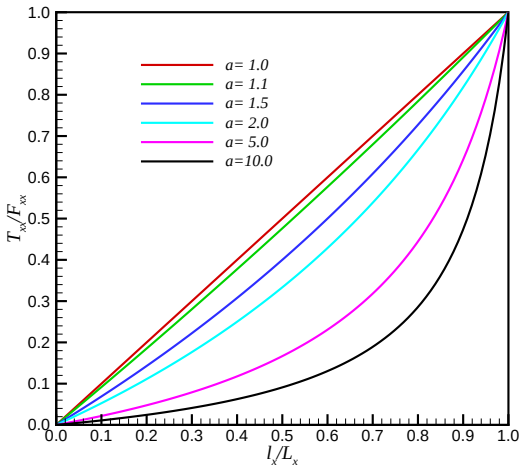

Figure 5 Stress stiffening efficiency varying with relative stiffness

The stiffening stress resultants N_{xx} and N_{yy} are shown in Fig. 6 where the boundary of the piezoelectric actuator is highlighted in black. Notice that N_{xx} is highly discontinuous along $x = 0$ and so is N_{yy} along $y = 0$. The discontinuities observed numerically are consistent with Eq. (12). Additionally, the region where there is compression in the x direction ($N_{xx} < 0$) is mostly limited to the region underneath the actuators. However, the same cannot be said about N_{yy}. This suggests that long piezoelectric film strips with large aspect ratios are able to orient stiffening stresses more efficiently than those with aspect ratios close to unity.

4 PIEZOELECTRIC STRESS STIFFENING AND BUCKLING

Considering that the membrane prebuckling problem given in Eq. (10) is satisfied, the FEM buckling equations can be derived from Eq. (7) to yield

$$\delta\Pi = \int_\Omega (\mathbf{M}^T \delta\boldsymbol{\kappa} + \mathbf{Q}^T \delta\boldsymbol{\gamma}) d\Omega + \int_\Omega (\mathbf{N} - \mathbf{F})^T \delta\boldsymbol{\epsilon}_N d\Omega. \tag{15}$$

The finite element method is used to solve the governing buckling problem Eq. (15). The element used is biquadratic depicted in Fig. 7 whose interpolation functions are:

$$\begin{array}{lll} N_1(\xi,\eta) = \frac{1}{4}\xi(\xi-1)\eta(\eta-1) & N_2(\xi,\eta) = \frac{1}{2}(1-\xi^2)\eta(\eta-1) & N_3(\xi,\eta) = \frac{1}{4}\xi(\xi+1)\eta(\eta-1) \\ N_4(\xi,\eta) = \frac{1}{2}\xi(\xi-1)(1-\eta^2) & N_5(\xi,\eta) = (1-\xi^2)(1-\eta^2) & N_6(\xi,\eta) = \frac{1}{2}\xi(\xi+1)(1-\eta^2) \\ N_7(\xi,\eta) = \frac{1}{4}\xi(\xi-1)\eta(\eta+1) & N_8(\xi,\eta) = \frac{1}{2}(1-\xi^2)\eta(\eta+1) & N_9(\xi,\eta) = \frac{1}{4}\xi(\xi+1)\eta(\eta+1) \end{array} \tag{16}$$

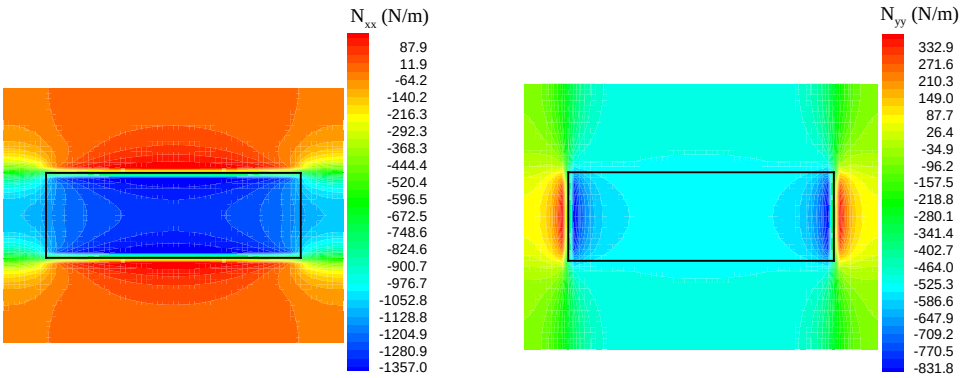

Figure 6 Stiffening stress distribution in terms of resultant forces

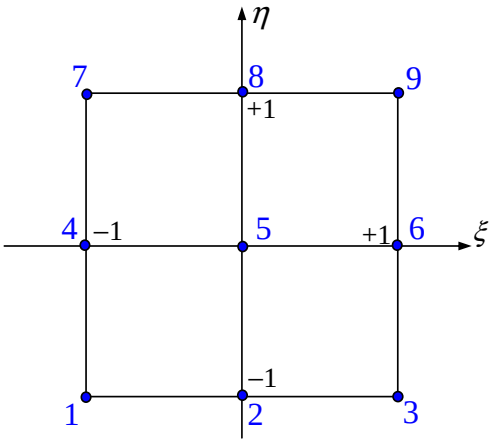

Figure 7 Biquadratic element

The interpolation functions given in Eq. (16) are used to interpolate five degrees of freedom per node: u, v, w, ψ_x and ψ_y. Hence the element contains a total of 45 degrees of freedom per element. When Eqs. (4), (5) and (16) are introduced into the first integral of Eq. (15) the finite element stiffness matrix $\mathbf{K}$ arises. The biquadratic element is less prone to shear locking than the traditional bilinear element. However, the reduced selective integration scheme is used to compute matrix $\mathbf{K}$. The second integral in Eq. (15) contains the membrane forces $\mathbf{N}$ and corresponds to a stiffening term (observe that it involves the nonlinear strains $\delta\boldsymbol{\epsilon}_N$). There are two types of contributions to $\mathbf{N}$: (i) the traditional mechanical stresses $\mathbf{N}_0$ due to N_{xx0}, N_{yy0}, N_{xy0}, and (ii) piezoelectric stiffening stresses $\mathbf{N}_p$ computed through solution of Eq. (10), such that $\mathbf{N} = \mathbf{N}_0 + \mathbf{N}_p$. Therefore, two geometric stiffness matrices arise: $\mathbf{K}_G^P$ from $\int (\mathbf{N}_p - \mathbf{F})^T \delta\boldsymbol{\epsilon}_N d\Omega$ and $\mathbf{K}_G$ from $\int \mathbf{N}_0^T \delta\boldsymbol{\epsilon}_N d\Omega$. Therefore, the complete FE buckling equation becomes

$$\left(\mathbf{K} + \sum_{i=1}^{p} \phi_i \mathbf{K}_{Gi}^{P} - \lambda \mathbf{K}_G\right)\mathbf{q} = \mathbf{0}, \tag{17}$$

where $\mathbf{K}$ is the stiffness matrix, $\mathbf{K}_{Gi}^{P}$ is the piezoelectric geometric stiffness matrix that incorporates the piezoelectric stiffening stresses and is associated with piezoelectric pair i, $\mathbf{K}_G$ is the geometric stiffness matrix, λ is the buckling load and $\mathbf{q}$ is the buckling mode. Notice that the formulation presented in Eq. (17) assumes that voltages of $\phi_i = 1$ V are applied in order to form matrix $\mathbf{K}_{Gi}^{P}$.

In order to obtain numerical results for buckling in the presence of piezoelectric stiffening stresses consider the plate used in the previous section ($L_x = 0.2$ m and $L_y = 0.15$ m) and one rectangular actuator with $l_x = 4$ cm and $l_y = 3$ cm placed in the center of the plate whose sides are parallel to the sides of the plate. Two types of traditional loadings are applied: (i) uniform compressive loading along the x direction (λ_{xx}) and uniform shear (λ_{xy}). The actuator voltage is varied within the limits of the depoling field, i.e., -50 V $\leq \phi \leq$ +50 V. Figure 8 presents the curves obtained for the $[0/90]_S$ and $[\pm 45]_S$ laminates. Points on those curves are obtained through solution of Eq. (17) for different values of ϕ. Buckling occurs under no mechanical loading (either $N_{xx0} = 0$ or $N_{xy0} = 0$) for some value of $\phi >$ +50 V for both types of loading. This conclusion agrees with the expectation that, when positive voltages are applied, compressive stiffening stresses, as those illustrated in Fig. 6, arise, impairing buckling behavior. The first buckling modes for the $[0/90]_S$ laminate subject to λ_{xx} are presented in Fig. 9 for different values of voltage. The differences between the mode shapes are not significant but the buckling load dramatically changes as seen in Fig. 8. However, the peaks of the normalized buckling modes, given in terms of transverse displacements w, become increasingly higher as the voltage is varied from -50 V to +50 V. The maximum $\lambda_{xx} = 660$ N/m and $\lambda_{xy} = 870$ N/m are associated with $\phi =$ -50 V. It can be observed that the $[\pm 45]_S$ laminate is less sensitive to variations in ϕ. This is evidence that sensitivity to ϕ is associated with the laminate lay-up. The $[\pm 45]_S$ laminate will suffer from buckling due to stiffening stresses only for value of ϕ substantially above +50 V.

A better understanding of Fig. 8 is gained if a perturbation analysis of the buckling eigenproblem is performed. Assume that the voltage of pair i is slightly perturbed by $\delta\phi_i$ such that the new eigenproblem derived from Eq. (17) becomes

$$\left[\mathbf{K} + \sum_{i=1}^{p} (\phi_i + \delta\phi_i)\mathbf{K}_{Gi}^{P} - (\lambda + \delta\lambda + \delta^2\lambda + ...)\mathbf{K}_G\right](\mathbf{q} + \delta\mathbf{q} + \delta^2\mathbf{q} + ...) = \mathbf{0}, \tag{18}$$

The zero-, first- and second-order problems derived from Eq. (18) are respectively

$$\left(\mathbf{K} + \sum_{i=1}^{p} \phi_i \mathbf{K}_{Gi}^{P} - \lambda \mathbf{K}_G\right)\mathbf{q} = \mathbf{0}$$

$$\left(\sum_{i=1}^{p} \delta\phi_i \mathbf{K}_{Gi}^{P} - \delta\lambda \mathbf{K}_G\right)\mathbf{q} + \left(\mathbf{K} + \sum_{i=1}^{p} \phi_i \mathbf{K}_{Gi}^{P} - \lambda \mathbf{K}_G\right)\delta\mathbf{q} = \mathbf{0}$$

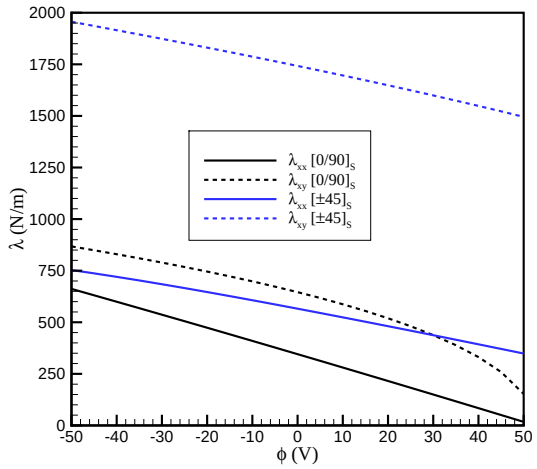

Figure 8 Buckling load vs. voltage: one patch parallel to plate's edges

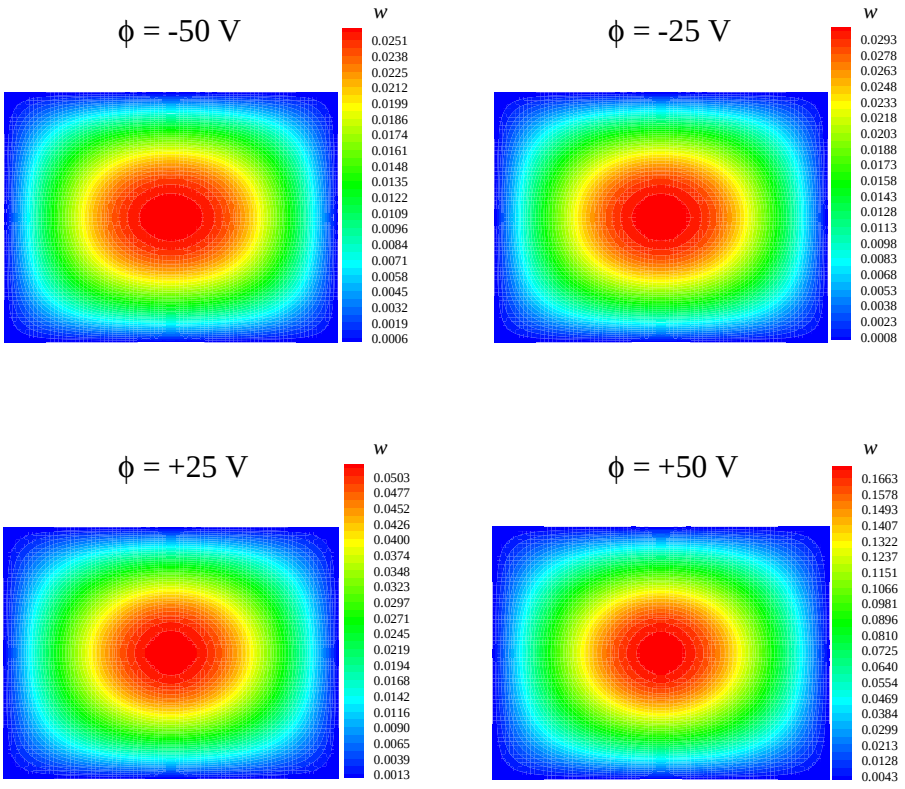

Figure 9 Buckling modes: $[0/90]_S$ laminate and λ_{xx} loading

$$\left(\sum_{i=1}^{p}\delta^2\phi_i\mathbf{K}_{Gi}^P-\delta^2\lambda\mathbf{K}_G\right)\mathbf{q}+\left(\sum_{i=1}^{p}\delta\phi_i\mathbf{K}_{Gi}^P-\delta\lambda\mathbf{K}_G\right)\delta\mathbf{q}+\left(\mathbf{K}+\sum_{i=1}^{p}\phi_i\mathbf{K}_{Gi}^P-\lambda\mathbf{K}_G\right)\delta^2\mathbf{q}=\mathbf{0}. \quad (19)$$

Multiplication of Eq. (19b) by $\mathbf{q}^T$ and using Eq. (19a) yields

$$\delta\lambda=\sum_{i=1}^{p}\frac{\mathbf{q}^T\mathbf{K}_{Gi}^P\mathbf{q}}{\mathbf{q}^T\mathbf{K}_G\mathbf{q}}\delta\phi_i. \quad (20)$$

Equation (20) shows that the sign of $\partial\lambda/\partial\phi_i$ is related to the the positive-definiteness of $\mathbf{K}_{Gi}^P$, $\mathbf{K}_G$ and the buckling mode $\mathbf{q}$. In the case of uniform compressive forces matrix $\mathbf{K}_G$ is positive-definite. However, the same cannot be said about $\mathbf{K}_{Gi}^P$. In fact, Fig. 6 indicates that the term $N_{xx}-F_{xx}$ is positive in some regions over the plate and negative over others. Hence, the sign of $\mathbf{q}^T\mathbf{K}_{Gi}^P\mathbf{q}$ depends ultimately on $\mathbf{q}$. Figure 8 just confirms this finding.

Multiplication of Eq. (19c) by $\mathbf{q}^T$ and using Eqs. (19a) and Eqs. (19b) yields

$$\delta^2\lambda=-\frac{\delta\mathbf{q}^T\left(\mathbf{K}+\sum_{i=1}^{p}\phi_i\mathbf{K}_{Gi}^P-\lambda\mathbf{K}_G\right)\delta\mathbf{q}}{\mathbf{q}^T\mathbf{K}_G\mathbf{q}}. \quad (21)$$

Matrix $(\mathbf{K}+\sum\phi_i\mathbf{K}_{Gi}^P-\lambda\mathbf{K}_G)$ is positive-definite provided buckling has not occurred. Therefore, the sign of $\delta^2\lambda$ given in Eq. (21) is certainly negative if $\mathbf{K}_G$ is positive-definite. Notice that this may not be the case when shear loadings are applied but it is true for the case where $N_{xx0}\neq 0$ and $N_{xy0}=N_{yy0}=0$. Figure 8 confirms that the concavity of the λ vs. ϕ curve is negative.

A network of piezoelectric actuators may be used to try to induce more favorable piezoelectric stiffening stresses. Figure 1b shows a possibility where the only patch shown in Fig. 1a is split into four smaller patches such that the total area is maintained constant. This procedure guarantees that, provided the same voltage is applied, the electric energy required is also the same. Figure 10 presents the λ vs. ϕ curves obtained assuming that equal voltages are applied to the four patches. Comparison to Fig. 8 leads one to conclude that the normal and shear buckling loads were decreased for both the $[0/90]_S$ and $[\pm 45]_S$ laminates. Therefore, this particular procedure did not bring any improvement to the buckling loads. However, this simulation suggests that the piezoelectric actuators should be placed as far from the boundaries as possible in order to boost the potential benefits of the piezoelectric stiffening stresses.

Figure 1c presents another possibility for placement of the actuators, i.e., patches with arbitrary orientation. In Fig. 1c the same rectangular patch of Figure 1a is used but it is oriented parallel to the plate diagonal. Figure 11 presents the λ vs. ϕ curves obtained. Comparison against Figs. 8 and 10 demonstrates that this configuration is the best one for both laminates whenever $\phi<0$ V and it has good performance for $\phi>0$ V except for extreme values of ϕ very close to +50 V. Hence, if permitted, the best strategy is to orient the patches along the diagonals, at least for the $[0/90]_S$ and $[\pm 45]_S$ laminates.

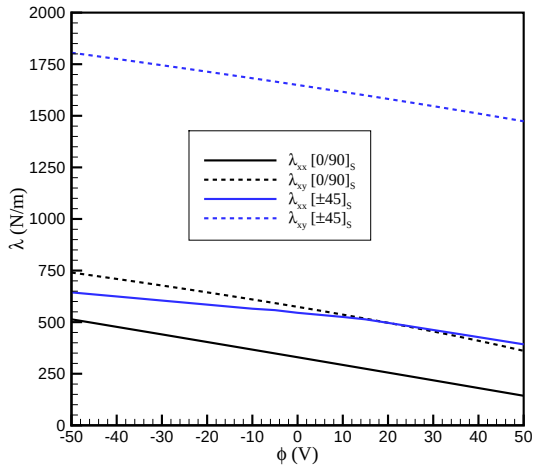

Figure 10 Buckling load × voltage: four patches parallel to plate's edges

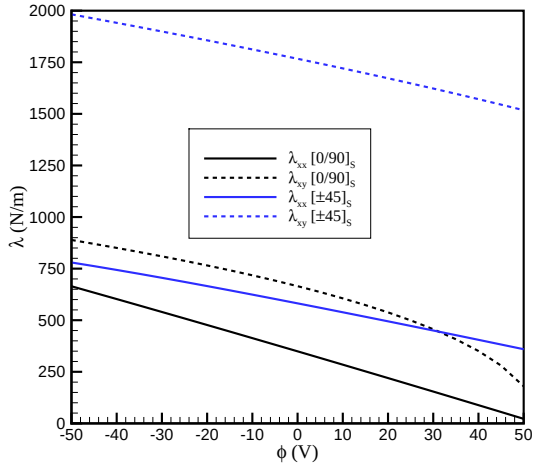

Figure 11 Buckling load × voltage: one patch parallel to plate's diagonal

5 CONCLUSIONS

This paper proposes the use of piezoelectric actuators to enhance buckling of composite plates through stress stiffening effects. An analytical approach to the prebuckling problem is pursued showing that discontinuities in the first derivative of displacements are expected to occur in the boundary of the plate separating domains with and without patches attached. This type of discontinuity can be effectively captured by plate or shell finite elements whose formulations are based on Mindlin assumptions. A tapered patch would certainly alleviate the discontinuity

jump but it consists in an impractical alternative from the experimental point of view.

The analytical solution obtained for the prebuckling regime is reasonable in the direction along which the piezoelectric patch is longer but yields unreasonable results in the shorter direction. Therefore, numerical procedures must be employed in order to obtain the precise distribution of piezoelectric stiffening stresses. Although not suitable for exact solution, Eq. (8e) contains a very important message: buckling cannot occur if there are no stiffening stresses $N_{xx} - F_{xx}$, $N_{yy} - F_{yy}$ or $N_{xy} - F_{xy}$. Therefore, it proves that free-free structures, even when equipped with piezoelectric actuators, will not buckle. The condition for the loss of stability is that either external mechanical loadings are applied or piezoelectric stiffening stresses arise as a result of boundary constraints.

Numerical simulations considered two symmetric laminates: $[0/90]_S$ and $[\pm 45]_S$. These were selected because the former is a typical lay-up in aeronautical construction and the later is the optimal lay-up against buckling in the normal direction (λ_{xx}). All the results show that buckling behavior is improved for negative voltages and is impaired for positive voltages. This is obviously a result of piezoelectric stiffening stresses over the composite plate. As a practical recommendation piezoelectric actuators should have their orientations carefully chosen, but the most important finding is that they should be placed as far as possible from the edges in order to maximize the beneficial effects of the piezoelectric stiffening stresses.

Acknowledgements This work was partially financed by the Brazilian agency CNPq (grants no. 300236/2009-3 and 303287/2009-8).

References

[1] R. C. Batra and T. S. Geng. Enhancement of the dynamic buckling load for a plate by using piezoceramic actuators. *Smart Materials and Structures*, 10(5):925–933, 2001.

[2] E. Carrera M. Boscolo and A. Robaldo. Hierarchic multilayered plate elements for coupled multifield problems of piezoelectric adaptive structures: formulation and numerical assessment. *Archives of Computational Methods in Engineering*, 14(4):383–430, 2007.

[3] K. Chandrashenkhara and K. Bathia. Active buckling control of smart composite plates - finite element analysis. *Smart Materials and Structures*, 2(1):31–39, 1993.

[4] E. F. Crawley and J. de Luis. Use of piezoelectric actuators as elements of intelligent structures. *AIAA Journal*, 25(10):1373–1385, 1987.

[5] A. R. de Faria. On buckling enhancement of laminated beams with piezoeletric actuators via stress stiffening. *Composite Structures*, 65(2):187–192, 2004.

[6] M. V. Donadon, S. F. M. Almeida, and A. R. de Faria. Stiffening effects on the natural frequencies of laminated plates with piezoelectric actuators. *Composites Part B: Engineering*, 35(5):335–342, 2002.

[7] S. V. Gopinathan, V. V. Varadan, and V. K. Varadan. A review and critique of theories for piezoelectric laminates. *Smart Materials and Structures*, 9(1):24–48, 2000.

[8] M. Kögl and M. L. Bucalem. A family of piezoelectric mitc plate elements. *Computers & Structures*, 83(15-16):1277–1297, 2005.

[9] C. K. Kundun, D. K. Maiti, and P. K. Sinha. Post buckling analysis of smart laminated doubly curved shells. *Composite Structures*, 81(3):314–322, 2007.

[10] T. Meressi and B. Paden. Buckling control of a flexible beam using piezoelectric actuators. *Journal of Guidance, Control and Dynamics*, 16(5):977–980, 1993.

[11] N. Y. Nye. *Physical Properties of Crystals: their representation by tensors and matrices*. Oxford University Press, 1972.

[12] J. N. Reddy. *Mechanics of Laminated Composite Plates: Theory and Analysis*. CRC Press, Boca Raton, 1997.

[13] M. Shariyat. Dynamic buckling of imperfect laminated plates with piezoelectric sensors and actuators subjected to thermo-electro-mechanical loadings, considering the temperature-dependency of the material properties. *Composite Structures*, 88(2):228–239, 2009.

[14] S. P. Thompson and J. Loughlan. The active buckling control of some composite column strips using piezoelectric actuators. *Composite Structures*, 32(1-4):59–67, 1995.